Life-Cycle of Structures and Infrastructure Systems – Biondini & Frangopol (Eds)

Nonlinear analysis of base isolated buildings with curved surface sliders including over-stroke displacements

Felice Carlo Ponzo, Antonio Di Cesare & Nicla Lamarucciola
University of Basilicata, Potenza, Italy

ABSTRACT: Seismic isolation represents one of the most suitable strategies for mitigating the seismic risk of structures and infrastructures. Acceptable probabilities of collapse for seismically isolated buildings could be achieved by an appropriate isolator displacement capacity. This paper investigates the effects of the over-stroke capacity of double concave curved surface sliding isolators, in addition to the nominal displacement capacity, on the seismic response of base isolated structures. The case study building is a reinforced concrete frame structure designed for high hazard seismic site. The level of performance of global collapse prevention has been investigated considering the earthquake intensity levels at the Collapse Limit State (with a return period of 1000 years). The results of the nonlinear static and dynamic analysis highlights that the seismic isolation without the over-stroke capability show a limited margin against collapse for seismic intensities beyond the design limit state level.

1 INTRODUCTION

The minimization of potential seismic damaging of a building can be achieved introducing flexibility at the base of the structure in the horizontal direction and damping element to reduce the amplitude of displacements. In recent years, one of the most widespread technologies is the seismic isolation, as a practical and economical alternative to traditional seismic reinforcement.

Nowadays there are many isolation devices that differ in construction technology, materials, geometry and operation. The most common seismic devices are elastomeric isolators and sliding isolation systems. The latter are composed of a certain number of moving parts (at least two) made of steel and composite materials which slide over each other expressing a specific friction force. One of the mainly used seismic isolation system is the Curved Surface Slider (CSS), also known as Friction Pendulum Slider® (FPS), firstly developed by Zayas (Zayas et al. 1987), which includes both re-centering and good dissipation capabilities being based on the pendulum mechanic principle.

The double CSS bearing (or Double Concave Curved Surface Slider - DCCSS) consists of two facing concave stainless-steel surfaces separated by a slider which can be either articulated or rigid. The DCCSS can be modelled as two CSS in series associated with same coefficient of friction μ and effective radius of curvature R_{eff} (Fenz & Constantinou 2006, Ponzo et al. 2017).

The CSS devices can be further divided in two main groups: devices with or without a displacement restrainer, which prevent the inner slider to slid past a certain point which usually is the perimeter of the housing pad. These elements can be for example displacement restraining rings, which are made of the same material of the housing plate and can be welded, bolted to it or even form a single block with the pad itself (Bao et al. 2018). Retaining elements such as restraining ring (Figure 1a) are widely used in America (Kitayama & Constantinou 2019) in order to control displacements and to avoid the isolator disassembly when displacements higher than the design ones occur. Anyways, the impact against such retaining elements may induce significantly high acceleration onto the superstructure. On the contrary, the European Standards (UNI EN 15129:2018) do not allow the presence of restraining end-stroke element that can be damaged in case of a seismic event higher than the Maximum Credible Earthquake (MCE) and only approves

DOI: 10.1201/9781003323020-174

the use of structural joints separating the superstructure from the surrounding constructions, in order to safely accommodate the seismic movement. In particular, the European Standard allows the use of ground retaining walls, (Figure 1b), or specific devices such as rubber bumpers attached to the walls, to be used as end-over-stroke. Usually in Europe, the gap separating the superstructure from the retaining wall is much larger than the displacement capacity of the isolators, and consequently, the inner slider can run on the edge of the sliding surfaces for earthquakes producing displacement larger than the isolators capacity. When displacement restraining elements are not employed, and concave plates feature a flat rim (Bao et al. 2018b), the inner slider movement beyond the geometric capacity displacement d_c of the isolator is allowed entering in the so-called over-stroke displacement regime. The slider running in the over-stroke displacement regime it is capable of providing the DCCSS device with an increased displacement capacity d_{lim} and sliding force (Di Cesare et al. 2019, Ponzo et al. 2020, Di Cesare et al. 2021, Ponzo et al. 2021, Furinghetti et al. 2021a). Figure 1 shows the DCCSS in two deformed conditions: with a restraining ring and with overstroke capacity and moat wall.

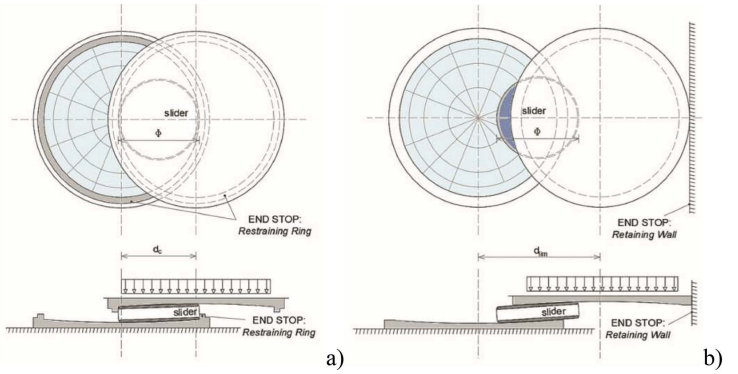

Figure 1. DCCSS bearing in deformed condition a) with a restraining ring d_c; b) with overstroke capacity and retaining wall $d_{lim} \geq d_c$; in plan and cross section view (Di Cesare et al. 2021).

The equations of motion and the limit displacements for the over-stroke sliding regime have been characterized by (Di Cesare et al. 2022, Furinghetti et al. 2021b) but a proper argumentation is needed in order to provide designers with the accurate displacement capacities and forces of DCCSS isolators.

This paper focuses on a case study of isolated building by means of DCCSS isolators with and without over-stroke displacement and moat wall, designed following the Italian seismic code (NTC 2018, Ragni et al. 2018). The building is a six-storey concrete frame structure assumed located in the city of L'Aquila (Italy) on soil class C. Nonlinear static and dynamic analyses were performed considering earthquake intensity levels at Collapse Limit State. Analyses results in terms of global drift and base shear are presented.

2 DESCRIPTION OF THE CASE STUDY BUILDING

The prototype structure considered in this study represents a typical residential RC-frame buildings located in L'Aquila, characterized by a regular plan of approximately 240 square meters and 6 stories above ground (Figure 2). The ground level height is 3.4 m while the other stories heights are 3.05 m. The building includes a staircase, designed with knee beams, and all stories have the same 25 cm-thick slab.

Infill panels have been considered as regularly distributed in plan and elevation, with different opening percentages. Infills dead loads have been considered in the design process. More details about RC structural members and masonry infills can be found in (Ricci et al., 2019).

In the base-isolated configuration, a supplementary RC base slab has been implemented below the ground floor columns (Figure 2). Elastic beams have been added at the base floor

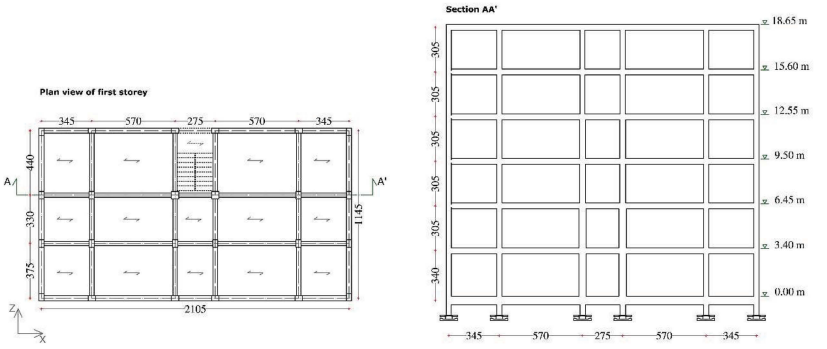

Figure 2. Case study building: plan view and longitudinal sections.

to realize the grid above the isolation system, consisting of 24 DCCSS isolators placed below the columns. Both concave plates of the DCCSS are characterized by the same radii of curvature and the same coefficients of friction ($R_1 = R_2$ and $\mu_1 = \mu_2$), and the assumed hypothesis is that sliding occurs simultaneously on both surfaces, considering a rigid cursor. The maximum displacement d_{max} has been assumed by catalogue, taking into account torsional effects, and the geometric capacity displacement d_c has been assumed as $d_c = 1.10 \cdot d_{max}$.

The total seismic weight W of the isolated frame is about 22380 kN and the vertical loads on the internal isolators N_{Sd} is about 1000 kN. The isolation system is designed considering the MCE spectrum shown in Figure 3a (UNI EN 1998-1:2004)

The seismic inputs considered in this study are reported in Figure 3b and consisted of a set of 20 ground motion for the intensity level corresponding to the Collapse Limit State (return period of 1000 years). The 5%-damped elastic spectra of the seismic records selected to represent the earthquake intensity level at MCE of the isolated structures is shown in Figure 3b. A reference period (conditioning period) closes to the design value of the fundamental period of vibration of $T = 3$ s has been considered. More details about the seismic hazard evaluation and the record selection for nonlinear dynamic analysis can be found in previous studies (Iervolino et al. 2018).

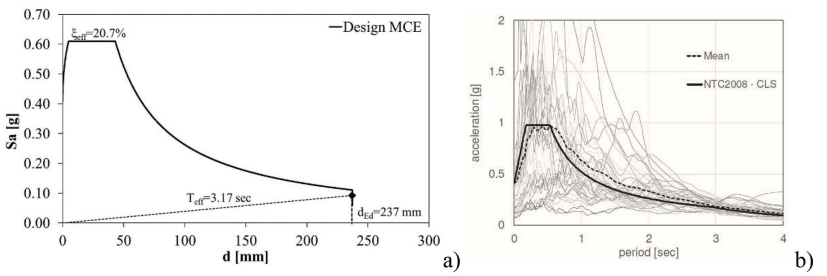

Figure 3. Acceleration response spectra of ground motion for Collapse Limit State (CLS) and Isolation systems design procedure on ADRS Spectra for LLS and CLS for L'Aquila site (Di Cesare, A., & Ponzo, F. C., 2023).

The geometric characteristics and main design parameters of the designed isolation system are reported in Table 1, in terms of: equivalent radius R_{eff}, friction coefficient μ, equivalent stiffness K_{eff}, effective period T_{eff}, effective damping ξ_{eff}, slider dimension, the maximum displacement d_{max}, the design displacement d_{Ed} of the isolation system at the MCE. For the over-stroke stage of motion the mechanical parameters are the increase of stiffness k_2 and friction coefficient $\Delta\mu$.

The oversizing due to the industrial discretization of the devices has been taken into account considering the ratio between the actual isolator displacement capacity d_c and the design displacement d_{Ed} equal to 1.4 in this study. The overstroke limit has been defined as the ratio between the ultimate displacement d_{lim} and d_c, equal to 1.25.

Table 1. Geometric characteristics and main design parameters of the isolation system at the CLS.

Case Study	R_{eff} [mm]	μ [%]	K_{eff} [kN/mm]	T_{eff} [sec]	ξ_{eff} [%]	d_{Ed} [mm]	Φ [mm]	d_{max} [mm]	d_c [mm]	d_{lim} [mm]
AQ_New	3700	2.5	0.357	3.17	21	237	200	±300	±330	±414

3 NUMERICAL MODELLING

The numerical model of the superstructure has been implemented in (OpenSEES 2006). A lumped plasticity approach has been considered for the structural elements of the superstructure, whereas elastic beams have been used for the base floor grid above the isolation system. The structural model also includes the staircase featuring inclined beams and cantilever steps. The cyclic degrading behaviour of plastic hinges (*modIMKmodel*) in the OpenSEES framework has been described implementing the model proposed by (Ibarra et al. 2005). In this study, 5% Rayleigh damping is used to model the viscous damping of the superstructure. Second order effects have not been considered. The masonry infills In-Plane (IP) behaviour has been modelled with an equivalent compression-only strut. The backbone curve of the diagonal strut has been defined on the basis of a modified version of the (Decanini et al. 2014) model, while the effect of openings has been taken into account through suitable strength/stiffness reduction factors. Both the Out-Of-Plane (OOP) and the IP/OOP interaction effects have been taken into account in the modelling strategy. Finally, local shear interactions, between masonry infills and adjacent RC columns, have been represented implementing shear springs at the ends of the columns to reproduce their nonlinear shear response triggered and amplified by the action of the adjacent equivalent compression-only diagonal. More information about superstructure modelling can be found in (Ricci et al. 2018).

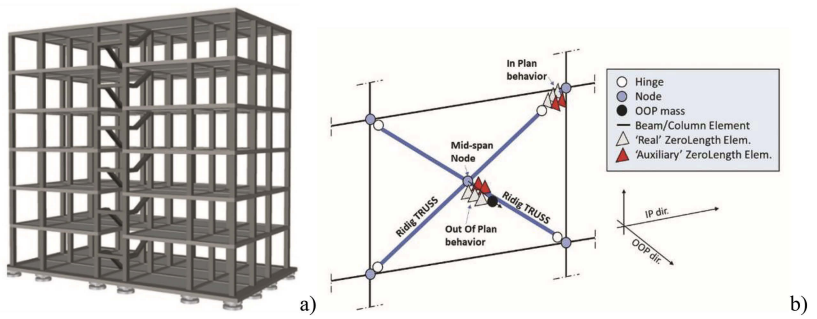

Figure 4. Schematical representation of the base-isolated prototype building and b) IP/OOP infill panels model.

The basic *SingleFPBearing* element (Figure 5) in OpenSees (OpenSees 2006) has been implemented to describe the DCCSS cyclic behaviour composed of a zero-length sliding hinge. The basic model has been modified in order to simulate the DCCSS behaviour during the over-stroke displacement, by adding three zero length parallel elements from the top *j-node* to a new fixed *k-node* (Figure 5). Two of these three zero length parallel elements have been modelled as elastic-perfectly plastic gap elements (*elasticPPGap*) defined by a gap displacement d_c, an elastic stiffness k_2, increased friction coefficient and a yielding force F_y, no hardening ratio or damage accumulation are considered so the gap material can recenter on load reversal. The last zero length element has been implemented considering a multi-linear elastic material (*elasticMultiLinear*), characterized by a nonlinear elastic behaviour without energy dissipation, defined by a set of stress-strain points.

The Rigid Gap has been modelled with a zero-length hinge, from j-node to s-node of Figure 5, consisting of an elastic-perfectly plastic gap element (*elasticPPGap*) with infinite stiffness ($k=\infty$) and at a gap displacement of d_C for models of rings or d_{lim} for models of rigid moat walls.

The ultimate displacement d_{lim} threshold value considered in the over-stroke regime is linked to the attainment of the first of the following conditions (Di Cesare et al. 2022): (i) vertical load instability; (ii) the displacement exceeds a limit value related to the maximum contact pressure between sliding interfaces (60 MPa) (iii) the device undergoes more than two over-stroke cycles. Plastic deformations of the end-stroke models, as example due to moat wall nonlinearity, were not taken into account. More details about numerical modelling of DCCSS in overstroke regime can be found in (Di Cesare et al. 2020, Ponzo et al. 2020, Di Cesare & Ponzo 2023).

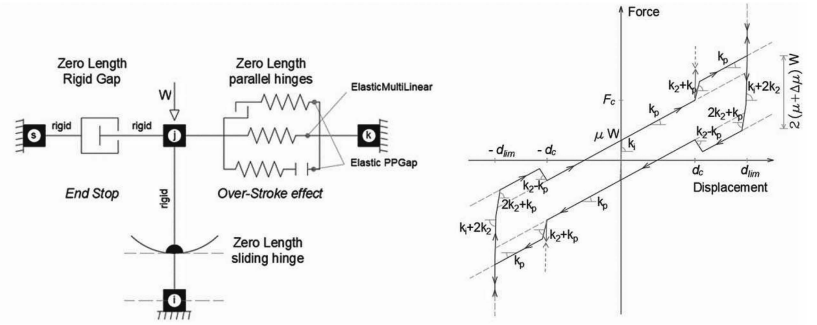

Figure 5. Spring model representation of the Modified SingleFPBearing with End-Stop and force vs displacement relationships for the retaining wall model.

4 NON-LINEAR STATIC AND DYNAMIC ANALYSES RESULTS

Nonlinear analyses have been performed considering different conditions of the isolation system. The seismic performance of the isolated structure and isolation system was evaluated by comparing the results of nonlinear static analysis (Pushover) in both horizontal directions with those of nonlinear dynamic analysis. A distribution of lateral forces proportional to the floor masses was used in the pushover analyses. In Figure 6 the pushover curves of not-isolated, base-isolated building, without and with overstroke and without and with rigid end-stop are compared. Pushover curves of base-isolated building model without displacement restraints (black dashed lines) show the basic behaviour of the isolation system, with a first quasi-rigid branch (pre-sliding stage), followed by a second branch accounting for isolators restoring stiffness. The isolated model with displacement restraints highlights a pushover behaviour of the not-isolated superstructure for displacement greater than the base displacement capacity d_c. In particular, as can be observed in Figure 6, for the configuration with isolation system and stop, after the pre-sliding stage and the second branch accounting for isolators restoring stiffness, the isolation system stops when the base displacement reaches d_c and superstructure pushover curve is shown again. The system with isolation system, over-stroke and stop perfectly overlaps the previous one for the first two branches, then, when the geometric capacity displacement is reached, the isolation system enters in the over-stroke regime with a third branch with increased stiffness friction force, and finally, when the end-over-stroke is reached (end of sliding), the superstructure pushover curve is shown again. It is possible to observe that the shape of the first part of the pushover curve of isolated structures can be approximated by an elastoplastic hardening behavior.

In order to evaluate the behaviour of the isolation system with and without rigid end-stop, the seismic response of base-isolated model has been investigated by means of multi-stripe nonlinear time-history analyses considering 20 real ground motions at intensity level corresponding to the collapse limit state and compared with pushover curves. The seismic input consisted of bi-directional horizontal ground motions time histories. In Figure 7 nonlinear dynamic results are expressed in terms of the acceleration displacement response spectrum, considering the maximum superstructure top displacement vs ratio between maximum base shear and total seismic weight. The dynamic results are in good agreement with the pushover curves both in sliding stage and in over-stroke stage. It is worth noting that the over-stroke regime has been reached

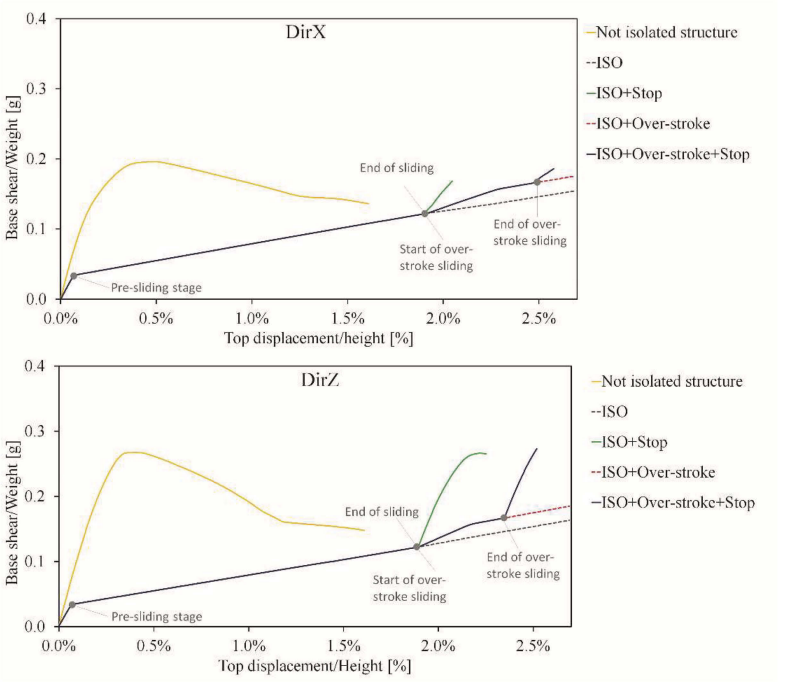

Figure 6. Pushover curves of not-isolated building and isolated with and without overstroke and with and without end-stop for horizontal directions.

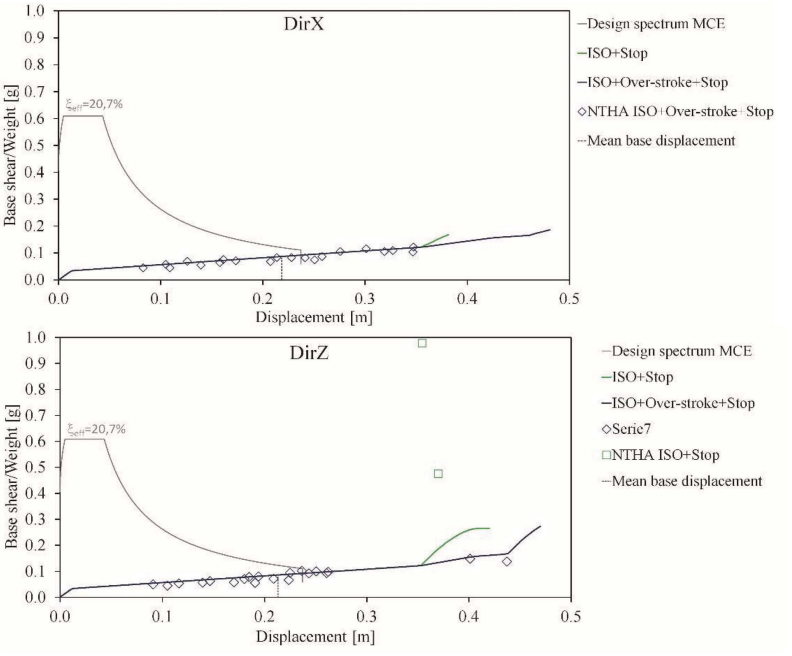

Figure 7. Nonlinear static versus nonlinear dynamic results in terms of maximum top displacement and acceleration at the base level for horizontal directions.

for two earthquakes of the spectra-compatible inputs, mainly due to the variability of the selected ground motion. For the same seismic inputs in the configuration with isolation system and rigid end-stop in the case of impact between the superstructure and the end stop dynamic analyzes provide values of the base shear significantly higher than those obtained from the push-over curves, due to the dynamic effects. Figure 7 also reports the mean values of maximum base displacements and the design MCE spectrum (see Figure 3b). The mean base displacement is slightly lower than the design displacement d_{Ed}.

5 CONCLUSIONS

In this paper a case study of a seismically isolated RC frame structure with DCCSS in high seismic zone was numerically investigated based on non-linear static and dynamic analyses. Coherently with commercially available DCCSS devices, the oversizing due to industrial discretization and the over-stroke displacement capacity of the bearings before reaching the end-stroke were considered. For the case of base isolation with overstroke, characterized by a ratio between the overstroke displacement d_{lim} and actual isolator displacement capacity d_c (d_{lim}/d_c) equal to 1.25, and by a ratio between d_c and the design displacement d_{Ed} (d_c/d_{Ed}) equal to = 1.4, non-linear dynamic analyses showed that the impacts against the end-stop are avoided in all seismic inputs spectra-compatible with the MCE. In all cases, the design displacement evaluated by equivalent static analysis and the mean value of maximum base displacement evaluated by nonlinear dynamic analysis are in good agreement.

Results from nonlinear static analysis and nonlinear time history analysis pointed out that over-stroke displacement of the isolators may significantly increase the safety factor in case of earthquakes bigger than the design ones, without drawing on the plastic resources of the superstructure and changing the construction costs. Further analyses are currently underway considering different case studies of retrofitted RC frame.

ACKNOWLWDGEMENTS

Authors would like to acknowledge the financial support of RELUIS 2022–2024 project (Work Package no. 15: Contributions to the Italian seismic code for base isolation and energy dissipation systems) funded by the Italian Civil Protection Department.

REFERENCES

Zayas, V.A., Low, S.S. & Mahin, S.A. 1987. The FPS earthquake protection system, *Earthquake Engineering Research Center*, Report, No. 87–01, Berkeley, California.

Fenz, D.M. & Constantinou, M.C. 2006. Behavior of the Double Concave Friction Pendulum Bearing. *Earthq. Eng. Struct. Dyn*, 35, 1403–1424.

Ponzo, F.C., Di Cesare, A., Leccese, G. & Nigro, D. 2015. Shaking table tests of a base isolated structure with double concave friction pendulum bearings. *Bulletin of the New Zealand Society for Earthquake Engineering*, 48(2), pp. 136–144

Bao, Y., Becker, T. C., Sone, T. &Hamaguchi, H. 2018. Experimental study of the effect of restraining rim design on the extreme behavior of pendulum sliding bearings. *EESD*, 47(4), 906–924.

Kitayama, S. & Constantinou, M.C. 2019. Effect of displacement restraint on the collapse performance of seismically isolated buildings. *BEE*, 1–20.

UNI EN. 15129:2018 2009. Anti-seismic devices. *European committee for standardization (CEN)*, Bruxelles, Belgium.

Bao Y, Becker TC, Sone T & Hamaguchi H. 2018b. To limit forces or displacements: collapse study of steel frames isolated by sliding bearings with and without restraining rims. *SDEE* 2018;112:203–14.

Di Cesare, A., Ponzo, F. C., Telesca, A., Nigro, D., Castellano, G., Infanti, S., et al. 2019. Modelling of the over stroke displacement of curved surface sliders using OpenSEES, *OpenSEES Days Eurasia*. Hong Kong.

Ponzo, F. C., Di Cesare, A., Telesca, A., Nigro, D., Castellano, M. G., & Infanti, S. 2020. Influence of DCCSS Bearings Over-Stroke and breakaway on the seismic response of isolated buildings. *Proceedings of the 17th World Conference on Earthquake Engineering*, September 2020, Sendai, Japan.

Di Cesare, A., Ponzo, F.C., & Telesca, A. 2021. Improving the earthquake resilience of isolated buildings with double concave curved surface sliders. *Eng. Struct*. 2280, 111498.

Ponzo, F.C., Di Cesare, A., Telesca, A., Pavese, A. & Furinghetti, M. 2021. Advanced modelling and risk analysis of RC buildings with sliding isolation systems designed by the Italian Seismic Code. *Appl. Sci*. 11, 1938.

Furinghetti, M., Yang, T., Calvi, P.M., & Pavese, A. 2021a. Experimental evaluation of extra-stroke displacement capacity for curved surface slider devices. *Soil Dyn. Earthq. Eng*. 146.

Di Cesare A, Ponzo FC & Telesca A 2022. Mechanical model of the overstroke displacement behaviour for double concave surface slider antiseismic devices. *Front. Built Environ*. 8:1083266. doi: 10.3389/fbuil.2022.1083266

Furinghetti, M. & Pavese, A. 2021b. Modeling strategies for the lateral response of curved surface slider devices under extreme displacement demands. *Proceedings of the COMPDYN 2021, 8th ECCOMAS Thematic Conference on ComputationalMethods in Structural Dynamics and Earthquake Engineering*, June 2021, Streamed from Athens, Greece.

NTC 2018. Italian technical code for constructions (in Italian). Ministry of Infrastructures, Italy 2018.

Ragni, L., Cardone, D., Conte, N., Dall'Asta, A., Di Cesare, A., Flora, A., Leccese, G., Micozzi, F. & Ponzo, F.C. 2018. Modelling and Seismic Response Analysis of Italian Code-Conforming Base-Isolated Buildings. *Journal of Earthquake Engineering*, Vol 22(2), doi: 10.1080/13632469.2018.1527263

Ricci, P.,Manfredi, V., Noto, F., Terrenzi, M., Petrone, C., Celano, F., et al. 2018. Modeling and seismic response analysis of Italian code-conforming reinforced concrete buildings. *Journal of Earthquake Engineering*, Vol 22, doi: 10.1080/13632469.2018.1527733

EN1998-1. Eurocode 8 2004. Design of structures for earthquake resistance—Part 1: general rules, seismic actions and rules for buildings. *European committee for standardization* (CEN), Bruxelles, Belgium.

Iervolino, I., Spillatura, A., & Bazzurro, P. 2018. Seismic reliability of code-conforming Italian buildings. *Journal of Earthquake Engineering* 22, 5–27. doi:10.1080/13632469.2018.1540372

OpenSEES 2006. Open system for earthquake engineering simulation. *PEER Center, University of California*, Berkeley. Available at http://opensees.berkeley.edu/.

Di Cesare, A., & Ponzo, F. C. 2023. Effect of Over-Stroke Capacity of Curved Surface Sliders on the Collapse Safety of Seismically Isolated Buildings. In *Seismic Isolation, Energy Dissipation and Active Vibration Control of Structures: 17th World Conference on Seismic Isolation* (17WCSI) (pp. 254–263). Cham: Springer International Publishing.

Ibarra, L.F., Medina, R.A., & Krawinkler, H. 2005. Hysteretic models that incorporate strength and stiffness deterioration. *Earthquake Engng Struct*. Dyn. 34, 1489–1511. https://doi.org/10.1002/eqe.495.

Decanini, L., Liberatore, L. & Mollaioli, F. 2014. Strength and stiffness reduction factors for infilled frames with openings. *Earthquake Engineering and Engineering Vibration* 13(3). doi: 10.1007/s11803-014-0254-9

Ponzo, F.C., Di Cesare, A., Telesca, A. & Nigro, D. 2021. Base isolated buildings with curved surface sliders including displacement restraints. In: *Proceeding of 14th World Congress in Computational Mechanics* (WCCM) ECCOMAS 2020, Virtual Congress, 11–15 Jan 2021.